THE PUBLISHING HOUSE
OF THE ROMANIAN ACADEMY

PROCEEDINGS OF THE ROMANIAN ACADEMY, Series A,
Volume 25, Number 2/2024, pp. 129–138
DOI: 10.59277/PRA-SER.A.25.2.07

FUEL-AIR RATIO EFFECT ON HYDROGEN-METHANE FLAMES IN A HIGH PRESSURE BURNER FOR GAS TURBINES

Sofiane OUALI

University M'Hamed Bougara UMBB of Boumerdes, Algeria,
Faculty of Technology, LEMI, Laboratory of Energy, Mechanics and Engineering
E-mail: `s.ouali@univ-boumerdes.dz`

Abstract. This numerical simulation studied the effect of H_2-CH_4 flame equivalence ratio on turbulent premixed combustion at 50%-50% concentration (by volume). The equivalence ratio was varied from 0.45 to 1.0 in 0.5 increments for 126 kW operating power, matching a 3.3 bar inlet reactant pressure. Tests utilized a gas turbine combustor. The thermal field, flow field, and pollutant emissions (NOx and CO) underwent rigorous analysis. The modelling framework applied steady Reynolds-Averaged Navier-Stokes (RANS) equations coupled to a probability density function (PDF) approach for turbulence-chemistry interactions and a NOx formation model.

Results showed increasing equivalence ratio from 0.45 to 1.0 elevated temperature approximately 900 K, significantly promoting NOx up to 1600 ppm and CO beyond 1900 ppm. However, equivalence ratio changes minimally impacted the overall flow field, maintaining stabilized flames. These findings provide new insight on thermochemical effects and flame stability in gas turbine (G.T) combustors across a range of equivalence ratios relevant for clean, high-pressure H_2-CH_4 combustion. The combined RANS-PDF methodology enables predictive simulation of turbulence, kinetics, emissions, and flame stability to guide optimal fuel-air ratio selection and low-emission combustor design.

Keywords: hydrogen, methane, turbulent combustion, premixed flames, gas turbines, combustor, pollutants.

1. INTRODUCTION

The growing demand for energy and environmental concerns have led the energy production industry to seek more efficient, eco-friendly solutions, particularly in G.T, which are vital for electricity generation and propulsion. One key strategy to enhance performance and reduce pollutants emissions involves optimizing reactive mixture combustion. Reactive mixture richness is a crucial factor affecting combustion behavior, with methane (CH_4) and hydrogen (H_2) mixtures being relevant choices.

This article focuses on the effect of mixture richness, specifically a 50% CH_4 and 50% H_2 mixture, in high-pressure swirl burners commonly used in gas G.T. The study aims to characterize performance and emissions variations across a richness range from 0.45 to 1 offering insight into the mixtures under realistic conditions.

The numerical simulations will analyze equivalence ratio variation effects on thermal field, dynamic fields and NOx and CO emissions. The burner's power is 126 kW at an operating pressure of 0.33 MPa.

The potential of H_2-CH_4 blends to reduce emissions and enhance efficiency has driven extensive investigations of combustion and emission characteristics across various practical contexts, including G.T, industrial burners, internal combustion engines, and more. Both experimental and computational studies have explored impacts on flame structure, stability, temperature profiles, chemical kinetics, and pollutants emissions such NOx and CO.

Several studies have revealed that hydrogen enrichment can substantially decrease emissions of CO, and CO_2 relative to pure hydrocarbon fuels (CH_4) due to higher flame speeds, low heating values (LHV), and adiabatic flames temperatures [1–7]. Numerical analysis of [1] reported over 90% reduction in CO through modeling of 60% hydrogen (by volume) in non-premixed methane combustion. However, emissions benefits can prove complex and depend on factors like equivalence ratio, pressure oscillations, burner geometry, injector design, and heat transfer rates [3, 7–9]. At higher concentrations, additional hydrogen beyond a critical threshold can introduce instability and revert emission decreases despite widening flammability limits, this implies an important tradeoff requiring further optimization [10].

Besides emission improvements, hydrogen addition has demonstrated combustion enhancements like shortened flame length, increased blowout resistance, and inhibited soot and flashback tendencies—though again proving dependent on specific configurations [2, 6, 11]. Fundamentally, hydrogen’s higher reactivity, diffusivity, and adiabatic flame temperature accelerate reaction rates and energy density relative to hydrocarbon fuels. This allows rapid, concentrated heat release beneficial for power generation and hybrid mixtures with CH_4 [8]. However, the intensified kinetics can also decrease residence time for products and inhibit complete fuel oxidation if not properly tailored, causing higher CO, unburnt hydrocarbons (UHC), and flame extinction [4, 9].

The complex dynamics illustrate the need to holistically optimize hydrogen integration for maximizing efficiency and stability while minimizing tradeoffs. Developing such optimized systems requires expanding beyond fundamental characterization to applied technologies experiencing increased hydrogen adoption, like GT, internal combustion engines, and industrial burners. Although literature has spanned swirl flames, upward combustors, acoustic interactions and simulations applied combustion contexts lack comprehensive insights into variable fuel mixture impacts [3, 7, 10].

This literature synthesis highlights the importance of controlling combustion parameters in industrial burners, especially when adopting novel fuels in systems initially designed for conventional combustibles.

This study aims to contribute to the scientific understanding of the technique involving the addition of H_2 to CH_4 in industrial burners. Given that GT manufacturers currently advocate for the substitution of H_2 up to 50% in existing GT (old models), the present work seeks to investigate the impact of H_2 on combustion. Furthermore, the introduction of H_2 to CH_4 inevitably entails a modification of the equivalence ratio of the reactive mixture. The specific objective of this work is to analyze the behavior of H_2-CH_4 flames over a sufficiently broad range of equivalence ratios (from 0.45 to 1).

This article is structured into four Sections. Section 1 serves as an “introduction”, providing context for the study along with a literature review. In Section 2, titled “Numerical Simulation”, the methods and approaches employed are comprehensively detailed. Section 3, “Results and Discussion”, the analyzes results: curves and fields of velocities, temperatures, as well as pollutant emissions. Finally, the article concludes with Section 4, offering a comprehensive conclusion of the work.

2. NUMERICAL SIMULATION

This study involves a 3D computational simulation of H_2-CH_4 (50%–50% by volume) flames in a swirled high pressure burner used in GT. The calculations were developed using ANSYS 17.2; Design Modeler for geometry generation, Fluent for simulation and CFD Post for results analysis. In selecting the software, the decision was grounded in its demonstrated capability to analyze reactive flows with exceptional precision, particularly in terms of turbulence and chemical kinetics.

2.1. Physical models

The predictive capability of the computational model stemmed from the specialized implementation of turbulence, combustion and emissions treatments tailored to the studied application. Careful selection of physical models enabled a comprehensive description of flames behavior. In this study, tree models were used: Realizable k-epsilon for turbulence, Probability density function (PDF) for combustion and NO model for pollutants.

2.1.1. Turbulence closer

The Realizable k-epsilon turbulence model [12] was used; it is a widely used Reynolds-Averaged Navier-Stokes (RANS) turbulence model in computational fluid dynamics (CFD). Developed to simulate complex turbulent flows, this model enhances the accuracy of predictions by incorporating realizable constraints, addressing certain limitations of the standard *k*-epsilon model. In the Realizable *k*-epsilon model, the two primary transport equations are solved for turbulence kinetic energy (k) and its dissipation rate (epsilon). The model introduces additional terms in the epsilon equation to ensure that the calculated dissipation rate adheres to certain realizability conditions, making the model more physically meaningful and accurate. It performs well in predicting boundary layer separation and vortex shedding. This makes it suitable for reactive swirling flows [13].

2.1.2. Combustion modeling

Partially premixed combustion systems were used to treat combustion. It involves premixed flames characterized by non-uniform fuel-oxidizer mixtures, as indicated by varying equivalence ratios [13]. The Chemical Equilibrium partially-premixed models operate under the assumption that the premixed flame front is infinitesimally thin, with unburnt reactants ahead and burnt products trailing behind the flame front. The flame-brush is characterized by a mean reaction progress variable "C" ranging from 0 for unburnt mixture to 1 for burnt mixture. Also, Zimont approach [14, 15] was used for the turbulence flame speed closure with Probability Density Function (PDF) [16] to treat chemical species distribution.

2.1.3. NO_x modeling

The NO_x model was used, this approach treats apparition of NO_x including NO and NO_2. It employs a detailed reaction mechanism to address the complexity of chemical reactions involved in NO_x formation accounting. The model uses the Fenimore prompt model [17] and Zeldovich mechanism [18].

2.2. Geometry

The computational geometry reproduced an experimental high-pressure swirl combustor design [19] representative of G.T. As depicted in Fig. 1, the burner comprises converging air passages feeding premixed fuel and air mixture to the combustion chamber. The cylinder length is 434 mm and the diameter is 100 mm. Swirl is generated from 9 radial fins ports at the inlet to enhance mixture and flame stabilization (Fig. 2).

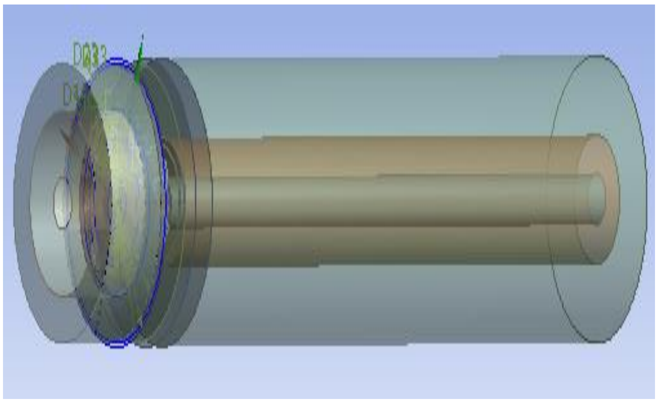

Fig. 1 – Geometry.

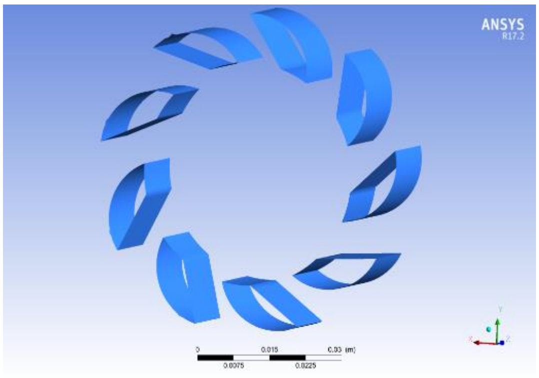

Fig. 2 – Swirler.

2.3. Mesh study

Figure 3 displays the computational mesh comprising quadrilateral elements at an axial section. Refinement levels were tailored to regions of steep gradients in physical flow variables near the inlet as well as wall boundaries to satisfy model resolution requirements and capture turbulence dynamics.

A grid independence study was conducted, evaluating axial velocity profiles over mesh densities ranging from 0.3 million to 2 million cells. As evident in Fig. 4, no variation was observed beyond 1.75 million nodes across the surveyed radial cross-section 50 mm downstream. This justified adopting 1.75 million grid for subsequent analyses.

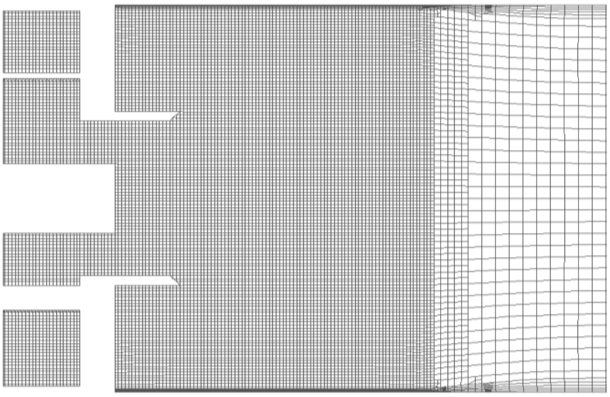

Fig. 3 – Grid structure.

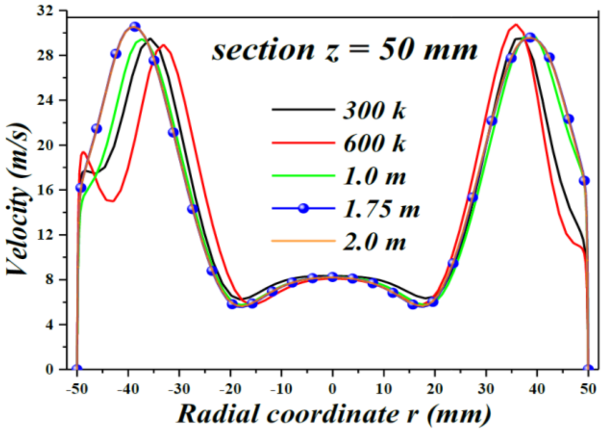

Fig. 4 – Mesh independency.

2.4. Operating conditions

The aim of this work is to exclusively analyze the impacts of varying the equivalence ratio ϕ of CH_4-H_2 premixed flames, ranging from 0.45 to 1.0 in increments of 0.5. To ensure this, all other parameters were kept constant. Table 1 lists the adopted operating conditions.

Table 1

Operating conditions

Parameter	LHV (kJ/kg)	Inlet *T* (K)	Inlet *P* (MPa)	Swirl number (S)	Power (kW)
Value	57.85	573	0.33	0.8	126

Table 2 illustrates the simulation parameters employed, correlating with the variation in the reactant mixture's richness; mass flow (MFR), chemical species mass fractions (MF), thermal conductivities (λ) and viscosities (η).

Table 2

Simulation parameters

ϕ	% MF CH_4	% MF H_2	MFR (g/s)	λ (J/m·K·s)	η (kg/m·s) (1e–05)
0.45	2.041	0.255	94.82876	0.0864	2.82
0.50	2.262	0.283	85.56367	0.0898	2.81
0.55	2.482	0.31	77.98313	0.093	2.8
0.60	2.701	0.338	71.66602	0.0955	2.78
0.65	2.919	0.365	66.32078	0.0988	2.77
0.70	3.135	0.392	61.73914	0.101	2.75
0.75	3.351	0.419	57.76838	0.104	2.74
0.80	3.565	0.446	54.29397	0.106	2.73
0.85	3.779	0.472	51.22831	0.109	2.71
0.90	3.991	0.499	48.50328	0.11	2.7
0.95	4.202	0.525	46.0651	0.113	2.69
1.00	4.413	0.552	43.87074	0.115	2.67

The equivalence ratio variation implies the use of Equation 1 and Equation 2 to calculate species mass fractions:

$$(1-\alpha)\mathrm{CH_4} + \alpha \mathrm{H_2} + \left(2 - \frac{3}{2}\alpha + x\right)(\mathrm{O_2} + 3.76\mathrm{N_2}) \rightarrow \text{combustion products} \qquad (1)$$

Here, α is the H_2 concentration by volume and *x* is determined as follow:

$$x = \frac{3}{2}\alpha + \left(\frac{2 - \frac{3}{2}\alpha}{\phi}\right) - 2 \tag{2}$$

In this study, three boundary conditions were employed:

– Burner inlet (pre-swirler valves): The "mass flow inlet" condition was applied, fixing both the inlet flow rate and the composition of the reactive mixture.

– Axial burner outlet: The "outflow" condition was implemented at the outlet, ensuring the conservation of the inlet flow rate.

– Burner walls: All burner walls were treated as "adiabatic" to precisely replicate the conditions of the experimental tests (without heat losses).

2.5. Validation

For the use of the combination of models cited in Section 2.1, a comparison of our results from numerical simulation was made with experimental results available in the literature [19, 20].

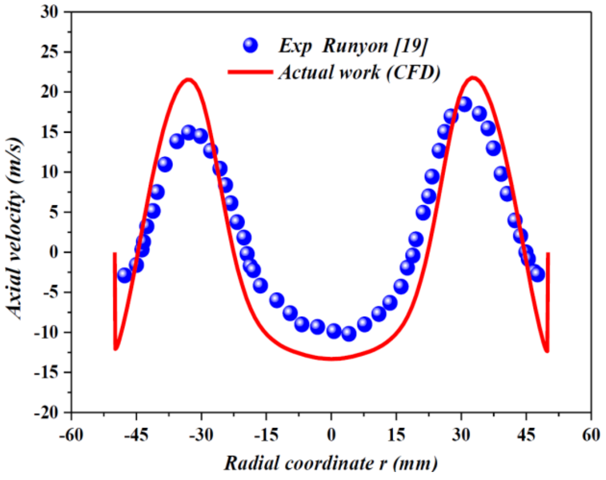

Fig. 5 – Velocity at $z = 32$ mm (radial cross-section).

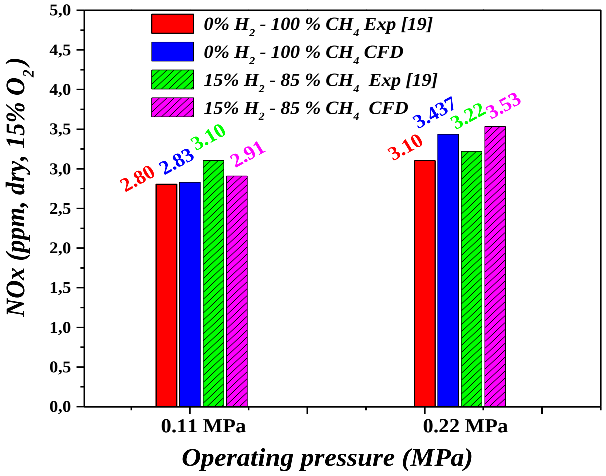

Fig. 6 – NO_x emissions for two powers.

Figure 5 shows profiles of axial velocity at $z = 32$ mm (radial-section) between the current simulation and experimental data [19], conducted at 126 kW of power (inlet pressure = 0.33 MPa). A favorable consistency is observed, wherein the Realizable *k*-epsilon turbulence treatment adeptly captures the intricacies of the flow field. The presence of both the central recirculation zone (CRZ) and outer recirculation zone (ORZ) aligns closely with experimental data, evidenced by regions exhibiting negative axial velocity. Peak axial velocities ($25\text{ mm} < r < 35\text{ mm}$), closely correspond as well. The minor variations between the simulation and experimental data are confined within reasonable limits. It is noteworthy that the relative error is maximally 10% at the center ($-15\text{ mm} < r < 15\text{ mm}$), while in regions where r ranges from 20 to 35 mm, the maximum relative error increases slightly to 12.5%. Overall, these results are acceptable and allow the use of this turbulence model.

Figure 6 depicts the NO_x emission rates as a function of burner power at an equivalence ratio of 0.55. Two power levels were investigated: 42 kW and 84 kW (corresponding to 0.11 MPa and 0.22 MPa, respectively). These tests were conducted for two different fuels: 100% CH_4 and 15% H_2–85% CH_4.

NO_x emissions were normalized and reported on a dry basis corrected to 15% O_2 per the ISO 11042-1:1996 standard [21]. Equation 3 and Equation 4 define the calculation procedure employed for this correction basis to comply with the calculation standards defined for G.T.

$$\mathrm{NO}_{x,\mathrm{dry}} = \frac{\mathrm{NO}_{x,\mathrm{mean}}}{1 - X_{\mathrm{H_2O}}} \tag{3}$$

$$\mathrm{NO}_{x,\mathrm{dry}}, 15\%\mathrm{O}_2 = \mathrm{NO}_{x,\mathrm{dry}} \cdot \left(\frac{20.9 - \mathrm{O}_{2,\mathrm{ref}}}{20.9 - \mathrm{O}_{2,\mathrm{mean}}}\right) \tag{4}$$

Here, $\mathrm{NO}_{x,\mathrm{mean}}$ is the molar concentration of NO_x (computed), $X_{\mathrm{H_2O}}$ is the H_2O MF, $\mathrm{O}_{2,\mathrm{ref}}$ is a referential concentration of O_2 in the air and $\mathrm{O}_{2,\mathrm{mean}}$ is the molar concentration (computed).

The obtained values (Fig. 6) exhibit excellent agreement between CFD-predicted NOx rates and experimental data [19, 20]. The maximum relative error is 10% (in the case of 100% CH_4 at 0.22 MPa), corresponding to 0.5 ppm. For other cases, the relative error ranges from 1% (100% CH_4 at 0.11 MPa) to 9% (15% H_2 – 85% CH_4 at 0.22 MPa). These results affirm the suitability of the selected mathematical models for our ongoing work.

The validation outcomes have motivated us to continue our study using the mentioned models. For the phenomena investigated here, this combination strikes a favorable balance between computational cost reduction and result accuracy. However, for more in-depth analyses, models demanding substantial computational resources (Large Eddy Simulation (LES), detailed chemistry, etc.) are requisite.

3. RESULTS AND DISCUSSION

3.1 Effect of equivalence ratio on thermal field

The variation in the richness of the reactive mixture ϕ directly affects the adiabatic flame temperature. This is why it is essential to meticulously investigate the effect of this variation on the thermal field.

Figure 7 shows steadily increasing temperature along the burner axis, spanning 1 500 K to 2 400 K, as equivalence ratio rises from 0.5 to 1.0. All studied cases sustained stable combustion, except for $\phi = 0.5$ where temperatures approached lean blowout limits around 1 500 K.

The positive trend between temperature and equivalence ratio is evident. A simulated case at $\phi = 0.45$ resulted in numerical flame extinction, requiring experimental investigations to conclusively determine lean stability limits for 50% H_2 – 50% CH_4 swirl flames. Defining operational boundaries for low-emission hydrogen-methane combustion aids development of sustainable aviation engines.

From $\phi = 0.55$ to 1, we observe stable and regular thermal fields, noting only that the increase in temperature inevitably leads to more significant pollution emissions. Also, it should be noted that long-term operation at high temperatures promotes the deterioration of the combustor.

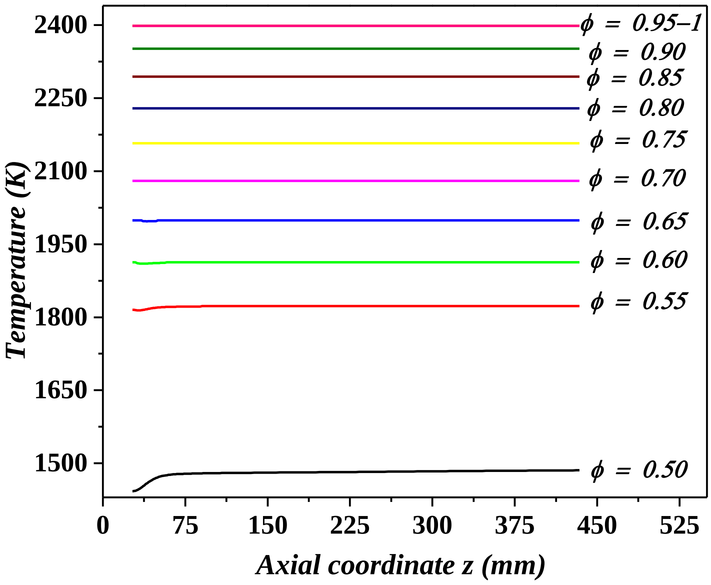

Fig. 7 – Equivalence ratio effect on temperature profiles.

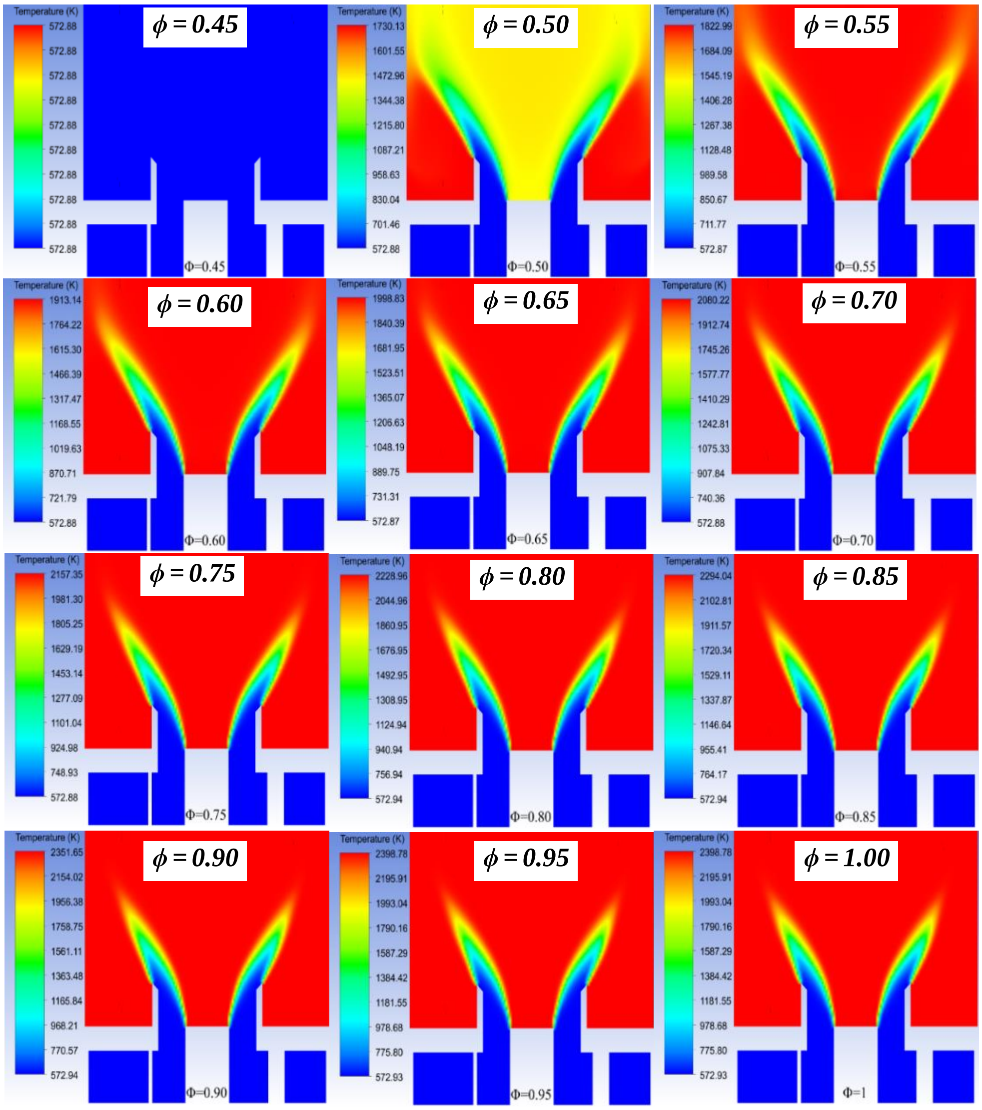

Fig. 8 – Equivalence ration effect on thermal field.

Figure 8 clearly illustrates thermal fields of the equivalence ratio ϕ variation. Results shows that for the first case (ϕ = 0.45), there is a total extinction of the flame. This prompts us to further investigate the lower mixture richness limits that should not be reached for CH_4-H_2 blend. The richness case of ϕ = 0.50 shows the existence of flames localized in the outer recirculation zones (ORZ) with a decrease in the reaction rate along the burner axis. This can be explained by the operating conditions where the mass flow inlet is more important than the other cases.

To maintain constant burner power, increasing equivalence ratio necessitates decreased reactant flow rates. Despite proportional temperature rises, the lower inlet velocities yield shorter flame lengths and reduced reaction zones. This manifests in more compact flame fronts. The decreased flame sizes could impact stability. While richness adjustments aim to preserve thermal input, the side effect of reduced flame volumes and increased reactions intensities must be counteracted to ensure operability.

3.2. Effect of equivalence ratio on dynamic field

Figure 9 illustrates the axial velocity profiles for several equivalence ratios ϕ at four radial cross-sections. Negative axial velocity values indicate the presence of recirculation zones that favor the heat release rate. The increase of axial velocity is inversely proportional to equivalence ratio. This is a direct result of the decrease in mass flow conditioned by the constant power maintenance.

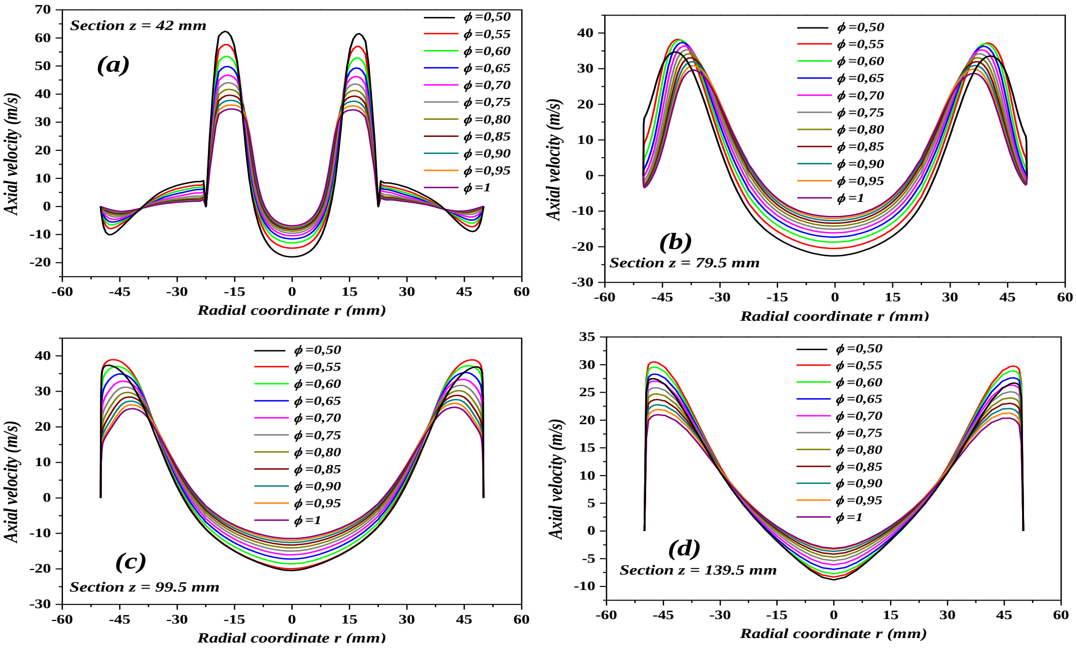

Fig. 9 – Equivalence ratio effect on axial velocity (at radial sections).

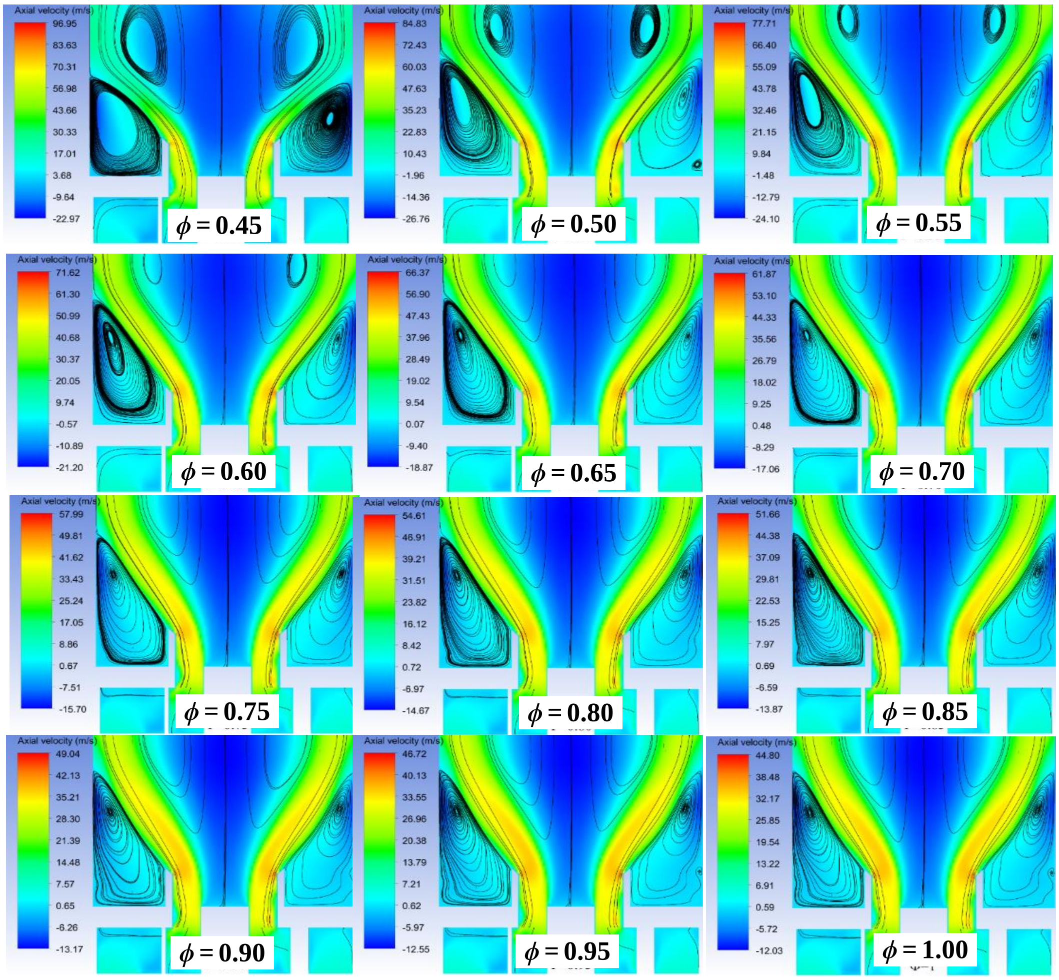

Fig. 10 – Equivalence ration effect on axial velocity fields (with streamlines).

Also noticeable, Fig. 10 shows the presence of two types of recirculation zones; a large central recirculation zone (CRZ) in the center of the combustor (–20 to +20 mm) and two smaller outer recirculation zones (ORZ) at the beginning of the burner.

Increasing equivalence ratio is also observed to reduce recirculation zone sizes due to lower reactant flow rates. A small outer recirculation zone (ORZ) appears in the lower combustion chamber corners for $\phi = 0.50$ case, affirming high velocities promote stabilization via vortex. As richness rises and velocities decrease, recirculation region scale diminishes. This suggests recirculation intensity should be considered during combustor sizing to enable flame holding, especially for ultra lean operation. Retaining adequate flow structures under varying thermal loads and equivalence ratios is imperative to ensuring operability across operating regimes.

3.3. Effect of equivalence ratio on pollutants emissions (NO$_x$ and CO)

In this numerical simulation, we examine the normalized emission rates of NO$_x$ (Equation 1 and Equation 2) and CO. CO is analyzed according to the previously cited standards [21] using Equation 5. For CO, it is not necessary to dehumidify it

$$\mathrm{CO, 15\%O_2} = \frac{20.9 - \mathrm{O_{2,ref}}}{20.9 - \mathrm{O_{2,mean}}} \cdot \tag{5}$$

Figure 11 illustrates the emission rate of NO$_x$ and CO as a function of richness in arranged ppm. The increase in richness of the mixture leads to a rapid increase in the emission rates of NOx and CO according to temperature increasing.

We notice an exponential rise from $\phi = 0.70$. Both pollutants start at almost zero values (1 to 3 ppm) and reach 1600 and 1850 ppm, respectively. These results show that the richness of the mixtures to be adopted should not exceed 0.65. Below these values, pollutant emissions are less than 50 ppm, which is very acceptable for burners with more than 120 kW of power.

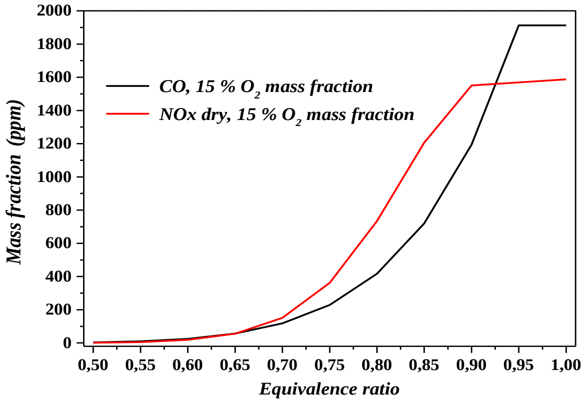

Fig. 11 – Equivalence ratio effect on NO$_x$ and CO emissions.

We can conclude that a mixture of CH_4-H_2 (50%–50%) is exploitable at moderate richness (between 0.55 and 0.65) to ensure flame stability and acceptable NO$_x$ and CO apparitions.

4. CONCLUSION

This numerical study investigated the impact of varying the equivalence ratio on the combustion characteristics of methane-hydrogen flames (50%–50% by volume) in a swirled GT combustor. The equivalence ratio was varied from 0.45 to 1.0 at a power level of 126 kW (corresponding to 0.33 MPa).

A mesh study and validation of the mathematical models employed were conducted. The selected model combination demonstrated notable accuracy while maintaining a very low computational cost.

Results revealed that under extremely lean conditions ($\phi = 0.45$), flame extinction occurred due to low flame temperatures and high mass flow inlet. For ϕ values between 0.50 and 0.65, stable flame operation was observed with acceptable NO_x and CO emissions (below 50 ppm). Increasing the equivalence ratio beyond 0.65 resulted in an exponential increase in NO_x and CO emissions, exceeding 1 600 ppm under stoichiometric conditions ($\phi = 1$).

The flame temperature increased proportionally with the equivalence ratio, ranging from 1 500 K at $\phi = 0.50$ to over 2 400 K at $\phi = 1$. Additionally, it was observed that the size of the central recirculation zone (CRZ) was inversely proportional to ϕ due to the reduction in mass flow rate. Flame stability was weakest at $\phi = 0.50$, attributed to a relatively high flow rate and a shortage of fuel in the local mixture composition.

In summary, 50%-50% CH_4-H_2 mixtures are suitable for high-pressure swirl burners in GT combustors within an equivalence ratio range of 0.55 to 0.65, producing stable and low-emission flames. Leaner conditions risk flame instability, while richer flames generate more pollutants. These findings are specific to the examined concentration (50% H_2–50% CH_4), and further tests are essential for generalizing these conclusions.

This work encourages the use of H_2 in existing GT by optimizing mixture concentrations and conducting preliminary tests regarding inlet flows, which significantly affect the resulting dynamic field and pollutant emissions.

REFERENCES

[1] Ilbas M, Yılmaz İ, Veziroglu TN, Kaplan Y. Hydrogen as burner fuel: modelling of hydrogen–hydrocarbon composite fuel combustion and NOx formation in a small burner. International Journal of Energy Research 2005;29(11):973–990.

[2] Kashir B, Tabejamaat S, Jalalatian N. A numerical study on combustion characteristics of blended methane-hydrogen bluff-body stabilized swirl diffusion flames. International Journal of Hydrogen Energy 2015;40(18):6243–6258.

[3] Shanbhogue SJ, Sanusi YS, Taamallah S, Habib MA, Mokheimer EM, Ghoniem AF. Flame macrostructures, combustion instability and extinction strain scaling in swirl-stabilized premixed CH4/H2 combustion. Combustion and Flame 2016;163:494–507.

[4] Cappelletti A, Martelli F. Investigation of a pure hydrogen fueled gas turbine burner. International Journal of Hydrogen Energy 2017;42(15):10513–10523.

[5] Rajpara P, Shah R, Banerjee J. Effect of hydrogen addition on combustion and emission characteristics of methane fuelled upward swirl can combustor. International Journal of Hydrogen Energy 2018;43(36):17505–17519.

[6] Alabaş B, Tunç G, Taştan M, Yilmaz I. Experimental investigation of the emission behaviour and flame stability of the oxygen and hydrogen enriched methane under acoustic enforcement. Fuel 2021;290:120047.

[7] Xin Y, Wang K, Zhang Y, Zeng F, He X, Takyi SA, Tontiwachwuthikul P. Numerical simulation of combustion of natural gas mixed with hydrogen in gas boilers. Energies 2021;14(21):6883.

[8] Karlis E, Liu Y, Hardalupas Y, Taylor AM. H2 enrichment of CH4 blends in lean premixed gas turbine combustion: An experimental study on effects on flame shape and thermoacoustic oscillation dynamics. Fuel 2019;254:115524.

[9] PASHCHENKO, D., Hydrogen-rich fuel combustion in a swirling flame: CFD-modeling with experimental verification. International Journal of Hydrogen Energy, 45(38), 19996–20003, 2020

[10] PATEL, V., & SHAH, R., Effect of hydrogen enrichment on combustion characteristics of methane swirling and non-swirling inverse diffusion flame. International Journal of Hydrogen Energy, 44(52), 28316–28329, 2019

[11] LI, Y., ZHANG, X., & WANG, Y., Experimental study on the combustion characteristics of premixed methane-hydrogen-air mixtures in a spherical closed chamber. Fuel, 299, 120885, 2021

[12] SHIH, T. H., LIOU, W. W., SHABBIR, A., YANG, Z., & ZHU, J., A new k-ϵ eddy viscosity model for high reynolds number turbulent flows. Computers & fluids, 24(3), 227–238, 1995

[13] Fluent, A. N. S. Y. S. (2016). Theory Guide 17.2. Ansys Inc USA.

[14] Zimont V, Polifke W, Bettelini M, Weisenstein W. An efficient computational model for premixed turbulent combustion at high Reynolds numbers based on a turbulent flame speed closure. In: ASME 1997 International Gas Turbine and Aeroengine Congress and Exhibition, vol. 78699. 1997, p. V002T06A054.

[15] Zimont VL. Gas premixed combustion at high turbulence. Turbulent flame closure combustion model. Experimental Thermal and Fluid Science 2000;21(1–3):179–186.

[16] Pope SB. PDF methods for turbulent reactive flows. Progress in Energy and Combustion Science 1985;11(2):119–192.

[17] Fenimore CP. Formation of nitric oxide in premixed hydrocarbon flames. In: Symposium on Combustion, vol. 13(1). 1971, pp. 373–380.

[18] Hanson RK, Salimian S. Survey of rate constants in the N/H/O system. Combustion Chemistry 1984:361–421.

[19] Runyon JON. Gas turbine fuel flexibility: pressurized swirl flame stability, thermoacoustics, and emissions [Ph.D. thesis], Cardiff University; 2017.

[20] Runyon J, Marsh R, Pugh D, Bowen P, Giles A, Morris S, Valera-Medina A. Experimental analysis of confinement and swirl effects on premixed ch4-h2 flame behavior in a pressurized generic swirl burner. In: Turbo Expo: Power for Land, Sea, and Air (American Society of Mechanical Engineers), vol. 50855. 2017, p. V04BT04A044.

[21] British Standard ISO 11042-1:1996. Gas turbines – Exhaust gas emission. Part 1: Measurement and evaluation, British Standards Institution, U.K.; 1996.

Received December 4, 2023